THE INFLUENCE OF INTERCELLULAR CLEFTS ON THE ELECTRICAL PROPERTIES OF SHEEP CARDIAC PURKINJE FIBERS

MARK SCHOENBERG, *Laboratory of Physical Biology, National Institute of Arthritis, Metabolism and Digestive Diseases, National Institutes of Health, Bethesda, Maryland 20014 and*

HARRY A. FOZZARD, *Departments of Medicine and The Pharmacological and Physiological Sciences, University of Chicago, Chicago, Illinois 60637 U.S.A.*

ABSTRACT A model of a 100-μm diameter Purkinje fiber with intercellular clefts was studied under voltage clamp conditions to examine the consequences of radial nonuniformity. Sodium and potassium conductances were distributed so that the surface and cleft membranes had similar channel density. Assuming that the model is appropriate, sodium current (and conductance) measured in the voltage clamp is grossly underestimated because of loss of voltage control of the cleft membrane. Under these conditions a value for $\bar{g}_{Na}$ of about 15–20 mmho/cm^2 of actual membrane is consistent with the experimental measurements of Dudel and Rüdel (1970. *Pfluegers Arch. Eur. J. Physiol.* **315**:136–158.). Intermediate and slow currents (slow inward current and potassium current) appear to be accurately measured under the model conditions, despite some voltage nonuniformity within the cleft. This result depended on the presence of a residual sodium current, and experimental removal of sodium may alter this result. All effects of nonuniformity would be accentuated in fibers of larger diameter.

INTRODUCTION

Although lengths of thin Purkinje fibers dissected from the walls of sheep heart behave much like simple one-dimensional cables (Weidmann, 1952; Délèze, 1970), their geometry is complex. A section of a 100-μm Purkinje fiber reveals it to be composed of about 6–12 cells in cross section, each with a diameter of about 40–60 μm and a length of 100 μm. Connections between cells are fairly common, appearing as gap junctions covering about 17% of the total junctional area (Mobley and Page, 1972).

The capacitance of a 100-μm diameter sheep cardiac Purkinje fiber measured by injecting step pulses of current is 12–15 μF/cm^2, when normalized by the apparent surface area (Weidmann, 1952; Fozzard, 1966; Schoenberg et al., 1975). The capacitance measured from the action potential foot, according to the technique of Tasaki and Hagiwara (1957), is only 2.4 μF/cm^2 (Fozzard, 1966). Fozzard (1966) suggested that the discrepancy could be resolved by assuming that two-thirds of the total capacitance measured with the square pulse technique was in series with a resistance of about 300 $\Omega \cdot$ cm. Sommer and Johnson (1968)

This work was presented in part at a symposium sponsored by the Muscular Dystrophy Association and the University of Rochester entitled "Membrane Control of Function in Excitable Tissues" held November 10–14, 1975 at the University of Rochester.

were instrumental in emphasizing the importance of geometry by pointing out that the membrane in series with a resistance was probably that portion of the cell membrane facing clefts between the cells making up the Purkinje fiber, as distinguished from the membrane on the surface of the cell bundle. The cleft membrane is continuous with the membrane on the surface, but current passing across it must also traverse the intercellular space. Since the individual cells are much longer than they are wide, this space appears as an intercellular cleft. If Sommer and Johnson are correct, then larger Purkinje fibers would be expected to have a larger capacitance per unit apparent surface area. That this is indeed the case was demonstrated by Schoenberg et al. (1975).

One model used to explain the effects of membrane not on the surface, but in series with the resistance of fluid in a narrow space, is the T-tubular model of Adrian et al. (1969), devised for frog skeletal muscle. This model assumes a constant capacitance per unit volume contributed by the T-tubules. A second type of model, in which the 100-μm Purkinje fiber was made up of six long, triangular cells arranged like six wedges of a pie, was put forth by Hellam and Studt (1974*a*) and Schoenberg et al. (1975). In this model, the membrane in series with a resistance was distributed along the six intercellular clefts. By comparison, the Adrian et al. model (1969) puts a larger fraction of the "internal" membrane nearer the surface, and that type of model for Purkinje fibers could not simultaneously account for both the amount of capacitance filled by the foot of the action potential and that measured by the square-wave technique.

Since the "pie-shaped" models of Hellam and Studt (1974*a*) and Schoenberg et al. (1975) explain the passive properties of Purkinje fibers reasonably well, and since little is known about the distribution of ionic currents between "surface" and "cleft" membrane in Purkinje fibers, it seemed reasonable to use the pie-shaped model as a tool for considering the effect of Purkinje fiber geometry upon recorded active currents. Our approach was to use a fairly simple model of ionic current channels in the surface and cleft membranes (just complicated enough so that the membrane could generate an action potential with overshoot and plateau), and then to see how the geometry of the clefts determined the currents that would be measured during a voltage clamp experiment. It was found that for the structural parameters measured by Mobley and Page (1972), the geometry of the fiber clefts influences the relationship between currents actually generated by the fiber membrane and those recordable during a voltage clamp experiment.

METHODS

A cross section of the simplified model for a 100-μm Purkinje fiber is illustrated in Fig. 1. The model is composed of six cells. The intercellular spacing is taken as constant (Sommer and Johnson, 1968) and in the "standard fiber" model has a value of 30 nm. We will refer to the sarcolemmal membrane directly on the surface as the overt membrane, and the sarcolemmal membrane situated in the clefts between cells as covert membrane. This covert membrane, although part of the surface membrane of a single cell, is not really at the "surface" of the fiber. Current passing through this membrane must flow through a resistance due to the finite conductivity of the fluid in the clefts. The overt and covert membranes are not perfectly smooth; they both have folds that make the real surface area larger than the apparent surface area. According to Mobley and Page (1972), this increase in area is 1.8-fold for the overt membrane and 3.6-fold for the covert membrane. Similar values have been reported by Hellam and Studt (1974*a*).

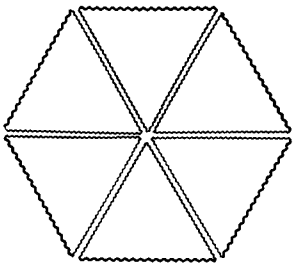

FIGURE 1 Model of a 100-μm-diameter Purkinje fiber. For the standard fiber, membrane folding causes the surface (overt) membrane to have an area 1.8 times the apparent surface area. The area of the covert membrane lining the clefts is increased 3.6-fold. The width of the clefts is 30 nm, and they are filled with fluid having a conductivity equal to that of Tyrode's solution. Membrane conductances and capacitances are described in text.

The particular arrangement of the cells and their shape in Fig. 1 were chosen because of the ease of mathematical treatment, and also because the apparent diameter of individual cells is 50 μm, the apparent surface to volume ratio of the cells is three times the apparent surface to volume ratio of the fiber, and the ratio of covert to overt membrane is 4 when the appropriate folding factors are taken into account. Mobley and Page (1972) reported a value of 0.114 μm^{-1} for the apparent surface to volume ratio of the cells, 0.037 μm^{-1} for the fiber apparent surface to volume ratio, and a value of 4.4 for the ratio of covert to overt membrane.

Our goal was to examine how the presence of intercellular clefts in the Purkinje fiber might influence the ability to study membrane currents by using a voltage clamp technique. More specifically, we addressed ourselves to the following question: if all the membrane in the Purkinje fiber, both overt and covert, had similar passive and active properties, would the current recorded during a voltage clamp experiment adequately reflect the current generated by the total membrane area if it were uniformly controlled at the clamping potential? In our analyses we were concerned solely with the influence of radial nonuniformities upon the recorded currents and did not study the influence of longitudinal nonuniformity, limited amplifier current, or microelectrode properties. These have been discussed elsewhere (Lederer and Tsien, 1976; Reuter and Scholtz, 1977; Fozzard and Beeler, 1975).

Since the influence of the clefts upon the currents recorded during a voltage clamp experiment depends almost exclusively upon the amplitudes and time constants of the various current components, rather than on the finer details of the current kinetics (see section on estimating voltage uniformity), we chose the simple model conductances suggested by Noble (1962) for most of the computations. The sodium current equations developed by Noble are modifications of those used to model the squid axon membrane, adjusted for the few known properties of the sodium current measured experimentally. These simple equations were chosen because they mimic much of the important behavior of the Purkinje fiber, including the ability to generate an action potential with a plateau, and also because they give current-voltage relationships not too different from those seen experimentally.

The experimental situation we are modeling is an ideal voltage clamp of a shortened Purkinje fiber, where the membrane potential controlled is that recorded by a micropipette placed intracellularly through the surface membrane relative to the external bath potential, with the assumption that the resistance of the bath fluid is small.

Symbols

I_s Total current across the surface membrane per unit length of "fiber" (μA/cm).

I_c Cleft current measured from, or injected into, a single cleft per unit length of fiber (μA/cm).

C_m	Capacitance per unit apparent membrane area from Noble, 1962 (μF/cm^2).
V	Membrane potential (mV).
V_r	Resting membrane potential (mV).
t	Time (ms).
I_{Na}, I_K	Sodium, potassium currents per unit apparent membrane area from Noble, 1962 (μA/cm^2).
m, h, n	Hodgkin-Huxley kinetic parameters.
η	Fraction of total membrane area that is on surface (overt). (Equal to 0.2.)
ϕ_c, ϕ_o	Linear folding factors describing degree of membrane folding of the covert and overt membranes, respectively (referred to as ϕ_i and ϕ_e in Mobley and Page, 1972).
a	Radius of "fiber."
x	Distance from center of fiber.
$\overline{G}_L, \overline{G}_m, \overline{C}_m$	Covert membrane passive parameters, defined and measured in Schoenberg et al. (1975).
$\tilde{G}_L, \tilde{G}_m, \tilde{C}_m$	Covert membrane passive parameters expressed per unit radial depth of cleft per unit length of fiber: $\tilde{G}_L = \phi_c \overline{G}_L/1$ cm; $\tilde{G}_m = \phi_c \overline{G}_m/1$ cm; $\tilde{C}_m = \phi_c \overline{C}_m/1$ cm.
I_{ic}	Active ionic current density of a single cleft (μA/cm^2 apparent surface area).

Surface Currents

The surface membrane current and conductances were defined by the following equations:

$$I_s/2\pi a = \eta[C_m(dV/dt) + I_{Na} + I_K] \tag{1}$$

$$I_{Na} = (400m^3h + 0.14)(V - V_{Na}) \tag{2}$$

$$I_K = (1.2n^4 + g_{K_1})(V - V_K) \tag{3}$$

$$g_{K_1} = 1.8 \exp[(V_K - V + 10)/50] + 0.015 \exp[(V - V_K - 10)/60] \tag{4}$$

$$dm/dt = \alpha_m(1 - m) - \beta_m m \tag{5}$$

$$dh/dt = \alpha_h(1 - h) - \beta_h h \tag{6}$$

$$dn/dt = \alpha_n(1 - n) - \beta_n n \tag{7}$$

$$\alpha_m = \frac{0.1(-V - 48)}{\exp[(-V - 48)/15] - 1} \tag{8}$$

$$\beta_m = \frac{0.12(V + 8)}{\exp[(V + 8)/5] - 1} \tag{9}$$

$$\alpha_h = 0.17 \exp[(-V - 90)/20)] \tag{10}$$

$$\beta_h = \frac{1}{1 + \exp[(-V - 42)/10]} \tag{11}$$

$$\alpha_n = \frac{0.0001(-V - 50)}{\exp[(-V - 50)/10] - 1} \tag{12}$$

$$\beta_n = 0.002 \exp[(-V - 90)/80] \tag{13}$$

$C_m = 12\,\mu$F/cm^2; $V_{Na} = +40$ mV; $V_K = -90$ mV.

The equations above are identical to those of Noble (1962) except in two regards. g_{K_1} has been

modified slightly to model a potassium concentration of 5.4 mM instead of a concentration of 4 mM. (At a concentration of 5.4 mM K, the model membrane is quiescent, whereas at 4 mM K it is spontaneously active). Also, all of the capacitances and conductances of Noble (1962) were multiplied by the factor η, as Noble's values were based upon all the membrane being overt. For the model of Fig. 1, only a fraction, η, equal to $6\phi_o^2/(6\phi_o^2 + 12\phi_c^2)$ is overt, where "6" and "12" represent the number of overt and covert surfaces and ϕ_o^2 and ϕ_c^2 are the folding factors that increase the membrane area (Mobley and Page, 1972). From Mobley and Page, $\phi_o = 1.35$ and $\phi_c = 1.9$, so that for our standard fiber, $\eta = 0.2$.

Cleft Currents

Schoenberg et al. (1975) derived equations that can be used to describe the clefts of the Purkinje fiber. By using the balance between transmembrane and intercellular (cleft) currents (intracellular radial currents were assumed to be small, since the diameter of the cells is large compared to the width of the clefts), they showed that a passive cleft with a geometry as in Fig. 1 could be described by the partial differential equation

$$\overline{G}_L[\partial^2(V - V_r)/\partial x^2] = \overline{G}_m(V - V_r) + \overline{C}_m[\partial(V - V_r)/\partial t], \tag{14}$$

where $\overline{G}_m$ and $\overline{C}_m$ are the conductance and capacitance per unit radial depth of 1-cm longitudinal length of cleft membrane, $\overline{G}_L$ is the conductivity per unit depth of the fluid in the cleft, x is the distance from the center of the cleft, and V_r is the resting potential. In Schoenberg et al. (1975), $\overline{G}_L = 3.1 \times 10^{-8}$ mho·cm, $\overline{G}_m = 0.3$ mmho/cm, and $\overline{C}_m = 5.5$ μF/cm are the probable values of these parameters in a 100-μm Purkinje fiber. $\overline{G}_L$, $\overline{G}_m$, and $\overline{C}_m$, as defined in Schoenberg et al. (1975), are the conductivity, conductance, and capacitance per unit depth for 1-cm length of cleft membrane. We may rewrite Eq. 14 in terms of $\tilde{G}_L$, $\tilde{G}_m$, and $\tilde{C}_m$, variables that represent the conductivity, conductance and capacitance, per unit depth per unit length of fiber, taking into account folding in the longitudinal direction. In this case $\tilde{G}_L = \phi_c\overline{G}_L/1$ cm, $\tilde{G}_m = \phi_c\overline{G}_m/1$ cm, and $\tilde{C}_m = \phi_c\overline{C}_m/1$ cm; Eq. 14 may be rewritten as

$$\tilde{G}_L[\partial^2(V - V_r)/\partial x^2] = \tilde{G}_m(V - V_r) + \tilde{C}_m[\partial(V - V_r)/\partial t], \tag{15}$$

where $\tilde{G}_L = 5.9 \times 10^{-8}$ mho, $\tilde{G}_m = 0.57$ mmho/cm^2, and $\tilde{C}_m = 10.5$ μF/cm^2. Defined in this way, $\tilde{G}_m$ and $\tilde{C}_m$ are the conductance and capacitance per unit apparent surface area of the passive cleft membrane. In the above equation, $\tilde{G}_m(V - V_r)$ represents the ionic current density through the "conductance channels" of the passive cleft membrane, as opposed to the current density discharging the membrane capacity $\tilde{C}_m\partial V/\partial t$. Therefore, in modeling Purkinje clefts with active membrane, we may write

$$\tilde{G}_L(\partial^2 V)/\partial x^2) = I_{ic} + \tilde{C}_m(\partial V/\partial t), \tag{16}$$

where I_{ic} is the ionic component of the active currents. To make the active membrane conductances in the cleft similar in form to those on the surface, we chose $I_{ic}\,\alpha(I_{Na} + I_K)$, where I_{Na} and I_K are defined by Eqs. 2 and 3. The constant of proportionality was taken as 0.85, a value that gave the clefts the same resting conductance as found by Schoenberg et al.

Comparison between Overt (Surface) and Covert (Cleft) Membranes

Since the parameters of the overt and covert membrane were defined from different starting points, it is useful before proceeding to compare their specific conductances and capacitances based upon real membrane area. The conductances chosen by Noble (1962) give a resting membrane conductance of 0.715 mmho/cm^2 apparent surface area. In our model we placed two-tenths of that in the surface membrane, giving a conductance for a covert membrane of 0.143 mho/cm^2 apparent surface area. This yields a specific conductance of $0.143/\phi_o^2 = 0.0785$ mmho/cm^2 real surface area. Similarly the specific capacitance of the overt membrane in our model, derived from Noble's value of 12 μF/cm^2

TABLE I

SPECIFIC CONDUCTANCE AND CAPACITANCE OF THE OVERT AND COVERT MEMBRANE OF THE STANDARD FIBER

Membrane	Specific conductance	Specific capacitance	Membrane time-constant
	mmho/cm²	*μF/cm²*	*ms*
Overt (surface)	0.079	1.33	16.9
Covert (cleft)	0.080	1.45	18.1

The values for the overt membrane are derived from Noble, 1962, while those for the covert membrane are from Schoenberg et al. (1975). The two are quite similar; the major difference is that Noble (1962) assumed a capacitance of 12 $\mu F/cm^2$ for a standard fiber. Schoenberg et al. found a value of 13 $\mu F/cm^2$ apparent surface area for a 100-μm fiber.

apparent surface area, is 1.33 $\mu F/cm^2$ real membrane area. The specific conductance and capacitance of the covert membrane are equal to $\tilde{G}_m/2\phi_c^2$ and $\tilde{C}_m/2\phi_c^2$, respectively, which yields 0.08 mmho/cm² and 1.45 $\mu F/cm^2$, as in Schoenberg et al. (The factor 2 results because both sides of each cleft are lined with membrane.) Table I summarizes these values along with the respective membrane time constants. The chosen properties of the overt and covert membrane per unit membrane are seen to be quite similar.

Solution of the Equations

Eqs. 1–13 for the overt membrane were easily solved on a Honeywell DDP-516 computer (Honeywell Information Systems, Inc., Waltham, Mass.), by using a standard fourth-order Runge-Kutta technique. Eq. 16 for the covert membrane was solved by a Crank-Nicholson finite difference approximation. The resultant tridiagonal matrix of equations was solved on a Honeywell DDP-516 computer using the Gauss elimination method (Smith, 1965). In practice the cleft was divided into 20 distance steps. If i and j represent the distance and time subscripts for each point in space and time, then each of the terms in Eq. 16, as well as Eqs. 2–4, could be written as

$$\partial^2 V/\partial x^2 \simeq \tfrac{1}{2}[(V_{i+1,j+1} - 2V_{i,j+1} + V_{i-1,j+1}) + (V_{i+1,j} - 2V_{i,j} + V_{i-1,j})]/(\Delta x)^2$$

$$\partial V/\partial t \simeq (V_{i,j+1} - V_{i,j})/\Delta t$$

$$V \simeq (V_{i,j+1} + V_{i,j})/2.$$

where Δx and Δt are the step sizes in space and time. α_m, β_m, α_h, β_h, α_n, and β_n, as well as g_{K_1}, are all expressed as functions of $V_{i,j}$. At $x = 0$, the center of the fiber or bottom of the cleft, we have the boundary condition that $\partial V/\partial x = 0$. At $x = a$, the surface of the fiber and cleft, the finite difference form of Eq. 16 has an additional term, $I_c/\Delta x$, on the right-hand side, where I_c represents the amount of current injected at the surface of each cleft per centimeter of fiber. The resulting series of equations can be solved under two conditions. Either I_c, the current injected, can be treated as the known variable and the equations used to solve for the voltage distribution along the cleft, or else the boundary condition, $V_{20,j} = V(a,t) = u_{-1}(t)[V_c - V_r]$, could be imposed at $x = a$, and the equations solved for I_c, as a function of time. The latter is tantamount to calculating the currents generated within the cleft and measured in response to a voltage clamp of the surface. The resulting voltage distribution along the cleft can also be calculated. This was the technique used in the present paper. For the model of Fig. 1, I_c was multiplied times six clefts.

In the section dealing with slow inward current, Eqs. 2–13 from Noble (1962) were replaced by the more complete set of equations describing the ionic components put forth by McAllister et al. (1975).

RESULTS

Passive Response

All of the computations performed were based upon the model illustrated in Fig. 1. The overt membrane was described by Eqs. 1–13 and the covert membrane by Eq. 16 (see Methods). Steady-state solution of these equations with $I_s = I_c = 0$ yielded a resting potential of −76.56 mV. For small hyperpolarizing voltage steps the "active" Purkinje fiber should give a passive response. The circles in Fig. 2 show the computed response of a single cleft of our "fiber" in response to a hyperpolarizing voltage clamp of the surface from the resting potential of −76.56 to −77.56 mV. This agrees well with the theoretical response described by Eq. 7*a* of Schoenberg et al. (1975) (solid curve). The close agreement between the two results demonstrates the accuracy and stability of the computer integration, at least in this voltage range.

Active Response

Fig. 3 shows a typical active response computed for a fiber like that in Fig. 1. Fig. 3 A shows the early currents and Fig. 3 B the late currents, in response to a voltage clamp from the resting potential of −76.56 mV to a potential of 0.0 mV. The solid curve shows the total current generated; the dotted curve shows the current generated by the surface membrane only. In the early record features of note include a large inward sodium current spike both on the surface and in the clefts. Preceding the sodium spike in the total current record is the "resistive-capacitative" current spike, designated by an arrowhead. This is the current necessary to discharge the capacitance near the mouth of the clefts to 0.0 mV. This has a nonzero

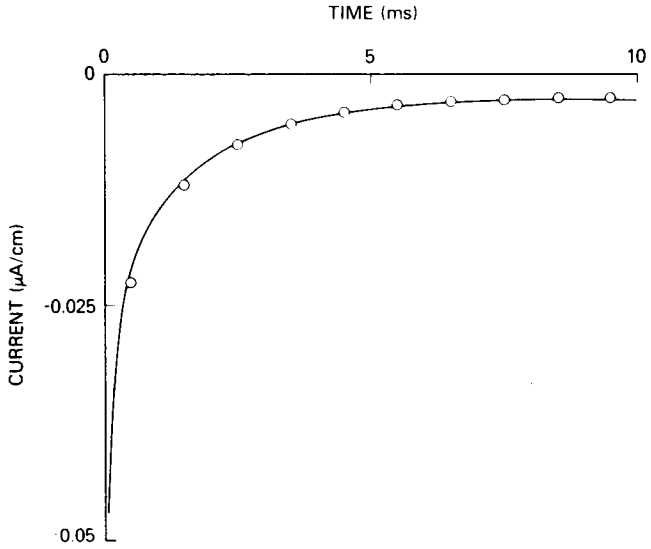

FIGURE 2 Comparison between analytic result and numerical integration procedure. Solid curve: analytic solution of the current response for a single cleft, 50 μm deep, voltage-clamped at its mouth from a resting potential of −76.56 mV to a voltage of −77.56 (Eq. 7*a* of Schoenberg et al., 1975). Circles: numerical integration solution of same problem using the techniques described in Methods for the standard fiber.

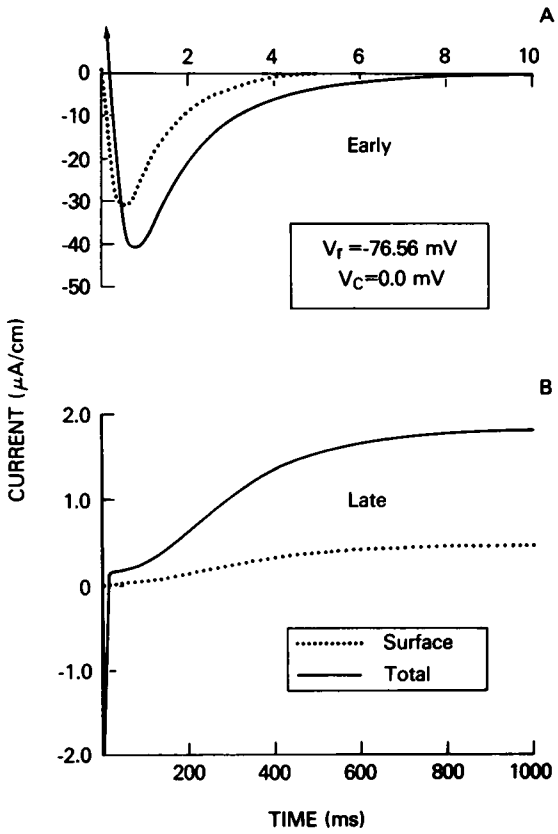

FIGURE 3 A typical computed response of a fiber like that of Fig. 1 to a depolarizing voltage clamp of the surface membrane. 3A shows the early, and 3B the later currents after a voltage clamp from a resting potential of −76.56 to a voltage of 0 mV. Solid curves: total current. Dotted curves: surface component only. Total current is the sum of the surface contribution plus that of the six clefts. Standard fiber.

duration because the current must flow across the nonzero resistance of the fluid within the clefts in series with the membrane. On the slower time scale record of the late currents, the sodium spike is greatly compressed and the major feature of note is an increase in current with time due to delayed rectifying properties of the K current. Quantitative analysis of the late currents in Fig. 3 B shows that for the example chosen, the total current is approximately equal to five times the surface current. Since the total area of membrane (overt plus covert) in Fig. 1 is five times the surface area, and since we selected approximately the same specific conductance (per unit area) for the surface and cleft membrane (see Table I), then the fact that the total current is approximately five times the surface current implies that the voltage distribution along the clefts is fairly uniform. That is, there is not a large voltage gradient between the cleft membrane near the surface and that near the center of the fiber.

Clamping the Membrane—Late and Intermediate Currents

Fig. 4 shows the magnitude of the late and intermediate (50 ms) clamp currents that would be recorded during a voltage clamp as a function of clamping voltage. For the 50-ms currents,

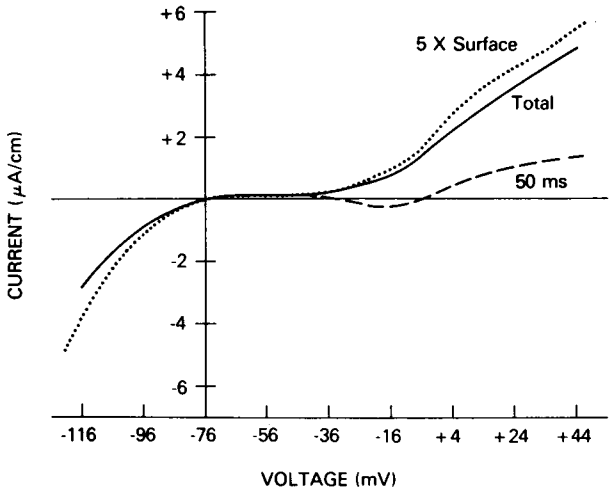

FIGURE 4 Current-voltage relationship of the late currents. Dashed curve: 50-ms current. Solid curve: total steady-state current. Dotted curve: five times the steady-state surface contribution. At 50 ms, five times the surface contribution is almost identical to the total 50-ms current. Standard fiber.

the total current is nearly identical to five times the surface current (dashed line). For the late currents, after the currents have grown significantly due to delayed rectification, the total current is still not very different from five times the surface current, even for large depolarizations. This suggests that almost all of the intermediate and late currents generated within the clefts would be recorded during a voltage clamp. It also implies, as discussed above, that the steady-state voltage distribution is still fairly uniform. The degree of voltage nonuniformity extant for the worst case over the range of Fig. 4, a voltage clamp to +44 mV, is shown in Fig. 5. At steady state, the depolarization from resting potential in the center of the fiber is still at least 80% of that on the surface.

Clamping the Membrane—Early Currents

Voltage clamping of the squid axon has proved to be a powerful tool for learning about early ionic currents. This is because it has been possible to hold the entire membrane area at reasonably constant voltage within a very short time after initiating the voltage clamp. In preparations such as frog skeletal muscle or the cardiac Purkinje fiber, the situation is more difficult because a large fraction of the muscle membrane is not in direct apposition to the low-resistance bath surrounding the fiber. We have already seen that the degree of voltage control achieved in the clefts by current injected through the surface membrane was reasonably adequate for recording intermediate and late currents. We consider here the ability to control the cleft voltage at short times, and the influence this has upon the recorded early currents.

Fig. 6 A shows the early clamp currents that would be recorded for a fiber, as in Fig. 1, for a hyperpolarizing clamp to −86.56. Note that the total current is approximately equal to five times the surface current after about 5 ms. This is the time necessary to establish voltage control of the passive cleft. (Fig. 2 and Schoenberg et al., 1975). Fig. 6 B shows the computed results for a large (101 mV) depolarizing clamp. In this case it takes some

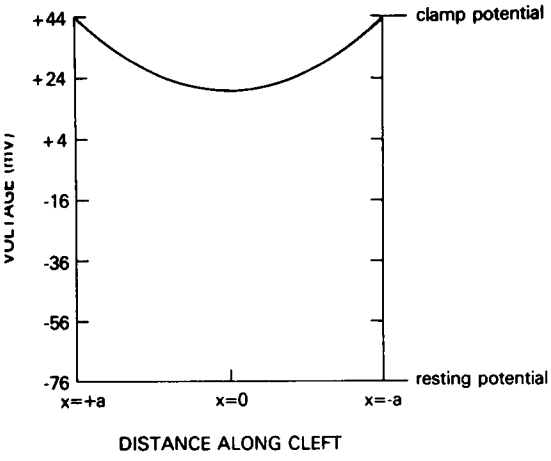

FIGURE 5

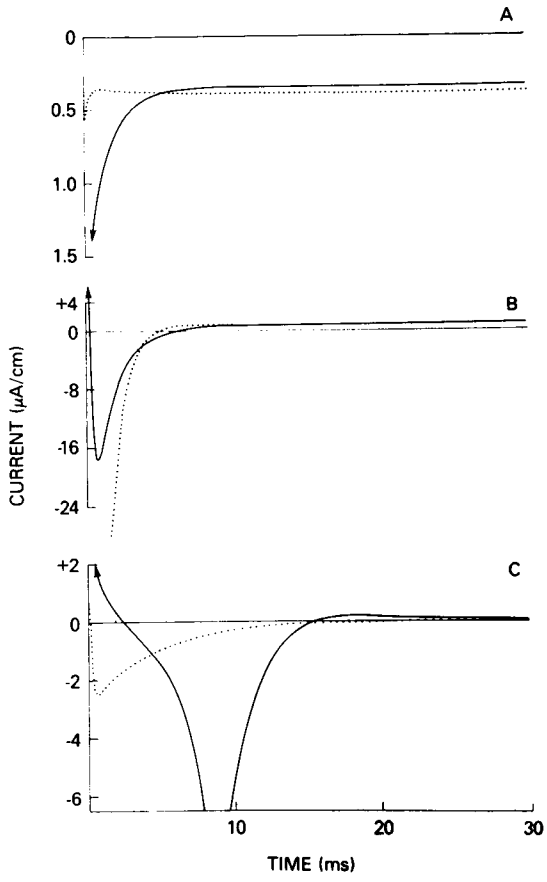

FIGURE 6

FIGURE 5 Steady state voltage distribution after a voltage clamp from resting potential of −76.56 mV to a potential of +44 mV. Standard fiber. Abscissa: distance along cleft. $x = 0$: center of fiber. $x = \pm a$: surface of fiber.

FIGURE 6 Early clamp currents. *A*: hyperpolarizing clamp to −86.56 mV. *B*: large depolarizing clamp to +24.44 mV. *C*: moderate depolarizing clamp to −56.56 mV. Standard fiber. Resting potential: −76.56 mV. Solid curves: total current. Dotted curves: five times surface contribution.

5–10 ms to establish voltage control. Fig. 6C shows a clamp to an intermediate voltage, $V = -56.56$. Very clear loss of control exists for some 15–25 ms. During this period there is uncontrolled sodium current activity in the cleft.

Attempting to Measure the Early Negative (Inward) Current

Fig. 7 shows the current-voltage relationships for the peak of the inward (sodium) current. It is divisible into at least two regions. In the region negative to −40 mV, for example at −56 mV, there is some evidence of uncontrolled sodium activity in the clefts while the surface membrane remains effectively clamped with very little regenerative sodium activity. In the region positive to −40 mV, we have a very different situation. Here not all of the current that could potentially be generated within the clefts is measured during the voltage clamp.

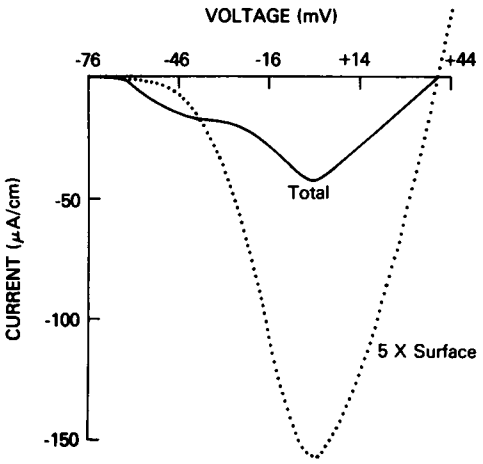

FIGURE 7

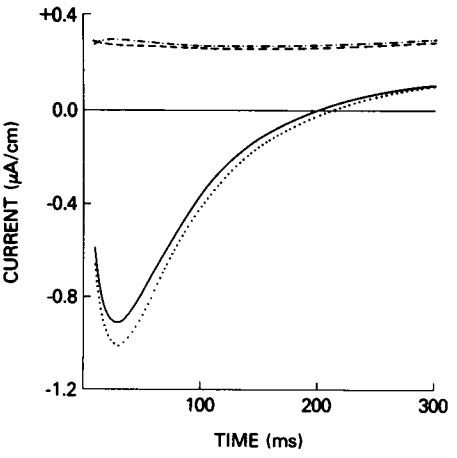

FIGURE 8

FIGURE 7 Current-voltage relationship for the peak of the early negative (sodium) current. Solid curve: total current. Dotted curve: five times surface contribution. Standard fiber.

FIGURE 8 Recording the slow inward current after a voltage clamp from a holding potential of −76.56 to −16.56 mV. The current components modeled according to McAllister et al. (1975). Solid curve (-): total current recorded during voltage clamp of fiber. Dotted curve (. . .): five times surface contribution. Dashed curve (- - -): total current from fiber with secondary inward current component of McAllister et al. set to zero. Dot-dashed curve (· -): five times surface contribution with secondary inward current set to zero. Curves illustrated from 10 ms. Before this, each curve would show a much larger negative spike related to sodium activity.

The net result is that the amplitude of the peak sodium current is drastically reduced; the total current recorded is roughly one-quarter what it would be if the clefts gave a contribution per unit area equal to that of the surface. In fact, the clefts, although they have four times as must area as the surface, produce one-quarter as much negative inward current.

There are at least four reasons why the net inward current for the entire fiber is not much greater than for the surface alone. First, the peak of the cleft current occurs later than that of the surface current, so that the peak of the total current is less than the sum of the peaks of the components. Secondly, the peak of the inward cleft current occurs some 2–5 ms after initiation of the voltage clamp. At this time, it is somewhat counterbalanced by the fairly large outward resistive-capacitative current that still exists. Thirdly, during the time when large negative currents are generated by the surface membrane, much of the cleft membrane is not generating large inward current because it cannot be controlled by the voltage clamp, and its potential has swung toward the sodium equilibrium potential, +40 mV. Near this potential very little sodium current is generated. Finally, during the time of sodium current generation, the cleft membrane length constant is very small, so that much of the current generated at the bottom of the clefts recrosses (as circulating current) the cleft membrane and does not appear at the bath ground where it would be recorded.

Measuring the Slow Inward Current

In addition to the large, rapid, inward current, another slower and smaller inward current is found in Purkinje fibers, which is measured after voltage clamps to intermediate voltages

(Reuter, 1967). It is interesting to consider whether this current, if generated both in the overt and covert membrane, could be measured accurately. Since the simple description of the ionic conductances put forth by Noble in 1962 did not contain this current component, we used the equations of McAllister et al. (1975) to address this question. Fig. 8 shows the resultant currents after a voltage clamp from a holding potential of -76.56 to -16.56 mV. Shown are the currents for the entire fiber and also for five times the surface contribution in the presence (lower curves), and absence (upper curves), of the secondary inward current component, in the equations of McAllister et al. (1975). It is seen in both instances that after the sodium spike (not visible in this figure), the total current is not too different from five times the surface current. As discussed earlier, this implies a relatively uniform voltage distribution along the cleft during generation of this current, and the ability to record the current generated fairly accurately.

We also computed the current responses after a voltage clamp to 0.0 mV, where an outward chloride current, in addition to the secondary inward current, is activated. In this instance, too, the total current was not very different from five times the surface contribution, the voltage distribution along the clefts was fairly uniform, and the secondary inward current could be accurately extracted from the records by subtracting the current response obtained in the absence of any secondary inward conductance from that obtained when all the conductances were present.

Estimating the Voltage Uniformity along a Cleft

We found the degree of voltage uniformity along a cleft for currents with time constants greater than 5–10 ms easy to estimate, once the approximate slope conductance of the cleft membrane was known. For these more slowly changing currents, capacitative charging of the membrane is less important, so that we may approximate Eq. 15 as

$$\tilde{G}_L[\partial^2(V - V_r^*)/\partial x^2] = \tilde{G}_m^*(V - V_r^*), \tag{17}$$

where $\tilde{G}_m^*$ is the approximate slope conductance per depth of the cleft per length of fiber, and V_r^*, the "quasi-resting potential," is the potential where the membrane current is zero. Both of these quantities may be obtained from the I–V relationship of the membrane, provided this function is not too complicated in shape. As an example we consider the question, "What is the voltage distribution along a cleft 50 ms after a clamp to -16.56 mV, if the cleft has conductances 100 times smaller and 100 times slower than those used in the standard fiber?" The current-voltage relationship for such a membrane at 50 ms is shown in Fig. 9. The current-voltage relationship near the clamping voltage of -16.56 mV can be approximated as illustrated by the dashed line in Fig. 9. $\Delta V = 20.3$ mV, so that $V_r^* = -16.56 - 20.3 = -36.86$ mV. $\Delta I = -13.3\ \mu A/cm^2$. Schoenberg et al. (1975, Eq. 6*a*) showed that the solution of Eq. 17, when $\tilde{G}_m^*$ is positive, may be written

$$V - V_r^* = \Delta V[\cosh(x/\lambda)/\cosh(a/\lambda)], \tag{18}$$

where x is distance from the center of the cleft, a is cleft length (fiber radius), and $\lambda = (\bar{G}_L/\bar{G}_m)^{1/2} = (\tilde{G}_L/\tilde{G}_m^*)^{1/2}$. When $\tilde{G}_m^*$ is negative, as in the present case, the solution is

$$V - V_r^* = \Delta V[\cos(x/\lambda)/\cos(a/\lambda)], \tag{19}$$

where $\lambda = (-\tilde{G}_L/\tilde{G}_m^*)^{1/2}$.

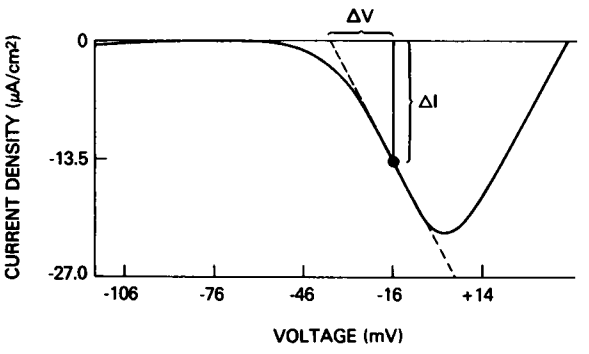

FIGURE 9

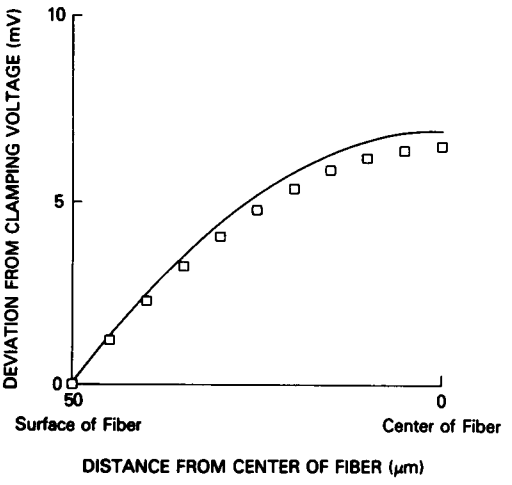

FIGURE 10

FIGURE 9 50-ms current-voltage relationship for a hypothetical current having conductances and rate constants 100 times smaller than those of the standard fiber. The current per apparent surface area at 50 ms (ordinate) is plotted versus clamp voltage (abscissa). The current-voltage relationship in the vicinity of −16.56 mV can be approximated as shown by the dashed line. $\tilde{G}_m^*$ for a cleft is equal to $2 \cdot (\Delta I/\Delta V)$, since each cleft is bounded on two sides by membrane. V_r^* is the voltage at the intercept of the dashed line and the zero current line.

FIGURE 10 Analytical approximation and computed solution for the voltage distribution along a cleft, 50 ms after a voltage clamp to −16.56 mV for a cleft with conductances as in Fig. 9. ΔV = 20.3 mV; V_r^* = −36.86 mV; $\tilde{G}_L = 5.9 \times 10^{-8}$ mho; $G_m^* = -1.31$ mmho/cm^2. Ordinate: deviation from clamping voltage (depolarization is +); abscissa: position from center of 50-μm radius fiber. Solid curve: analytic approximation; squares: computed results.

Fig. 10 shows the close agreement between the analytic approximation (Eq. 19) and the computed voltage distribution at 50 ms for the current described above. If the rate constants for this current had not been slow relative to the rate constant for changing the cleft voltage, the analytic approximation would not have been as adequate.

We do not know a priori the slope conductance of the clefts. However, as a practical matter, we may first use the above equations, assuming all of the conductance is in the clefts. This gives a "worst case" approximation with regard to voltage uniformity along the clefts. If this predicts a relatively uniform voltage distribution during measurement of a given current, we can assume that such a current, generated in the clefts, would be accurately measured during a voltage clamp. This type of argument suggests that both the potassium current and the slow inward current would be reasonably accurately recorded, even if they were generated in part by the covert membrane. This conclusion holds only for a Purkinje fiber with geometrical properties similar to Fig. 1. An increase in fiber diameter, a decrease in cleft width, or a decrease in lumen conductivity will all serve to diminish the ability to record these currents accurately.

Independence and Superposition

Consideration of the fiber model of Fig. 1 demonstrates that if a Purkinje fiber has currents generated from covert membrane, then it is difficult to make use of the principles of superposition and independence of currents. This is demonstrated by the fact that the sum of the

sodium current recorded in the absence of potassium (case I) and the potassium current recorded in the absence of sodium (case II), after a voltage clamp to a given voltage, is not equal to the total current recorded after a voltage clamp to the same voltage when both currents are present (case III). The reason for this is twofold. Firstly, a certain amount of current in case I and case II goes to discharge the membrane capacitance in the cleft, and the sum of these two is not necessarily the current needed to discharge the cleft capacity in case III. (If the voltage distribution is not too different, the resistive-capacitative currents (cases I, II, and III) are about equal.) Secondly, the presence or absence of various ionic conductances affects the voltage distribution along the clefts, which influences the current produced by the cleft. This effect is small when there is little voltage gradient down the cleft and large when it is great. Figs. 11 and 12 illustrate this effect. Fig. 11 shows the voltage distribution down a cleft in the presence and absence of sodium. To magnify the effect, the calculations were made for a fiber with a cleft length of 100 μm (200-μm diameter fiber), rather than 50 μm, as used for all the other calculations. Fig. 12 shows the effect of the difference in voltage distribution in the presence and absence of sodium upon the delayed rectifying current. This current, defined in our model as the steady state current minus the 50-ms current, is solely due to the potassium current, and is generated largely in the clefts. Although in the equations we have used, the potassium conductance is independent of the sodium conductance, it is clear that sodium conductance does indeed have a secondary effect that manifests itself through influencing the voltage distribution along the cleft.

DISCUSSION

Although the model used in these studies is a simplistic one, it reflects accurately some of the complex geometrical properties of the cardiac Purkinje fiber. Its distribution of membrane capacitance and resting conductance is based upon the cable studies of Schoenberg et al. (1975) and is consistent with the analysis of Hellam and Studt (1974*b*). In its main

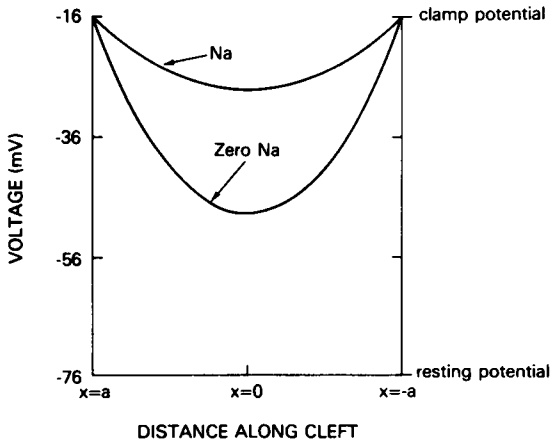

FIGURE 11 Steady-state voltage distribution after a voltage clamp to $V = -16.56$ mV in the presence and absence of sodium. Parameters as in standard fiber except fiber radius, a, = 100 μm and $I_{N_a} = 0$, in case without sodium. Abscissa: distance along cleft; $x = 0$, center of fiber; $x = \pm a$, surface of fiber. Note increased voltage nonuniformity in absence of sodium conductance.

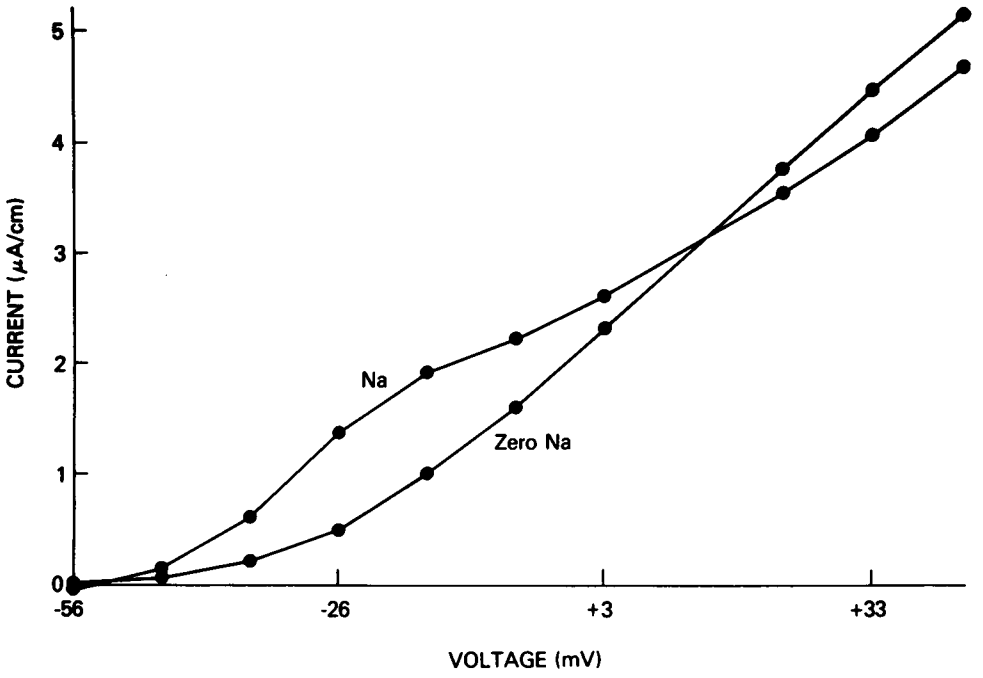

FIGURE 12 Effect of sodium removal upon delayed rectification. Fiber model as in Fig. 11. Delayed rectifying current (ordinate) is defined as steady-state current minus 50-ms current. Abscissa: clamp voltage.

features, it resembles the anatomical descriptions of several reports (Sommer and Johnson, 1968; Mobley and Page, 1972; and Hellam and Studt, 1974*a*). It is multicellular, has intercellular clefts with dimensions similar to those reported, and has the appropriate ratio of overt to covert membrane.

Some assumptions in the model certainly must represent oversimplifications. The clefts were assumed to have a constant width of 30 nm, as reported by Sommer and Johnson (1968). The estimate of Mobley and Page (1972) was 15–30 nm. Hellam and Studt (1974*a*) reported that the cleft width was quite variable, and averaged about 40 nm. If the variability in cleft width is not distributed systematically with regard to radial position, then the model may properly use the average value when the length constant of the cleft is large compared to its depth, or when cleft variability is not exceedingly great. If the variability in cleft width is as large as reported by Hellam and Studt (1974*a*), then the present model may require modification. Special gap junctional regions (nexuses) do represent points of constriction of the cleft. While no direct measurements are available for the shape of these junctional structures, the mean length of cleft membrane occupied by nexuses was reported by Hellam and Studt (1974*a*) to be 4.2%. If the nexuses are of this dimension, then they probably play little role in determining the effective resistance of the cleft.

The conductivity of the fluid in the clefts was taken as equal to that of Tyrode's solution. Although a reduction of this by 30–50% would not qualitatively change the results presented here, there are several reasons for choosing this as the appropriate value in the absence of hard experimental evidence. The conductivity of fluid inside Purkinje clefts or skeletal

muscle tubules is not precisely known because this parameter is derivable from experiments only once the geometry of the cleft or tubular network is precisely known. In the least complicated preparation studied, the transverse tubule of the tubular muscle fibers of a scorpion, the conductivity of the fluid in the tubule was derived to be equal to that of the bathing medium (Gilai, 1976). In the more complicated geometry of the frog skeletal muscle system, the analysis of Mathias et al. (1977), based upon the morphometric data of Mobley and Eisenberg (1975) and Eisenberg and Peachey (1975), derived a conductivity for the fluid in the tubular system 0.5–1 times that of the bathing medium. For the Purkinje fiber, Schoenberg et al. (1975) showed that a value of conductivity of fluid inside the cleft equal to that of the bathing medium gave a reasonable value for the capacitance filled by the foot of the conducted action potential, as well as the appropriate time constant for charging the clefts. In any case, the important characteristic is the apparent resistance to radial current flow in the cleft, a composite of the cleft width and the cleft conductivity.

We have not attempted an accurate description of Purkinje fiber currents, but instead have explored how currents representative of those recorded will be influenced by fiber geometry. The membrane ionic conductances used were similar in form to those of Noble (1962). An important property of those conductances is an instantaneous inward rectifying channel. This causes the K conductance to fall with depolarization to voltages between -70 and -20 mV, tending to increase the apparent length constant of the clefts and improve voltage uniformity. On the other hand, the time constants of the sodium activation variable are fast, a property that tends to increase voltage nonuniformity during the first few milliseconds. With rapid sodium activation, the surface responds more quickly than the clefts, which are delayed because of the time required to displace the charge on their capacitance. The use of the 1962 Noble equations in these calculations was arbitrary, but not unreasonable. They mimic satisfactorily the speed of onset of the action potential depolarization. The equations used by McAllister et al. (1975) result in a faster activation of the sodium current, and would lead to an even greater discrepancy between actual and recorded inward current.

One of the dramatic demonstrations of this model is that even if the covert membrane in a Purkinje fiber had an active sodium conductance, much of the current generated by it would not be recorded at the surface. For example, in Fig. 7 the discrepancy was as large as fourfold. When we reduced the time constants of the currents we used by 10-fold, so that they more closely resembled the time-course of currents in the cooled Purkinje fibers used by Dudel and Rüdel (1970), the discrepancy was only reduced to 3-fold (unpublished calculations). It therefore appears likely that sodium conductance in the clefts would be difficult to record even in cooled fibers.

The size of the discrepancy between generated sodium current and that recorded depends not only upon the rate constants of the current, but also somewhat upon the magnitude of $\bar{g}_{Na}$. It is therefore somewhat difficult to know the proper value for $\bar{g}_{Na}$ to use in modeling. In our model we used the Noble (1962) value of 400 mmho/cm^2, referred to the right-circular cylinder approximation of area. We distributed this conductance between the surface and the clefts so that the specific sodium conductance was about 44 mmho/cm^2, based upon actual membrane area. Dudel and Rüdel (1970), in their experiments in cooled fibers, obtained an estimate of 53 mmho/cm^2 referenced to the right-circular cylinder or 5.8

mmho/cm^2 of actual membrane. Increasing this value threefold in accordance with our modeling of the underestimation for cooled fibers would result in a value of 17.4 mmho/cm^2 actual membrane in the cooled fiber.

This value is similar to that used by McAllister et al. (1975) in their more recent model of Purkinje fiber currents at 37°C. It is somewhat smaller than the value of 44 mmho/cm^2 we have used, although reducing $\bar{g}_{Na}$ in our model to 15–20 mmho/cm^2 would have little effect upon the main conclusions. The most striking effect would be a still greater discrepancy between sodium currents generated and those measured at 37°C, since the positive resistive-capacitative current would be relatively larger (unpublished computations).

In contrast to the difficulties in recording sodium currents, our results suggest that most of the potassium current that could be generated by the covert membrane of the Purkinje fibers would be recorded accurately. However, the accurate measurement of potassium currents depended to some extent on the finer details of the model. An increase in radial nonuniformity was seen when sodium conductance was removed from the membrane, because the small, steady-state sodium current assists in depolarizing the depths of the cleft. This change in uniformity could result in distortions of the potassium I–V relationship. While the effect seen here as a result of the artifact was relatively small, it is interesting to speculate on the possibility that this might contribute to the change in threshold for delayed rectification in Na-free solution, as described by McAllister and Noble (1966). The artifactual alteration in the I–V curve depends strongly on the exact location of the m and h curves on the voltage axis (overlap), so that the importance of this artifact is impossible to estimate from available information.

Currents with intermediate kinetics were also investigated by using the ionic conductances of McAllister et al. (1975). A fair agreement was found between the total recorded current and that which would have been generated by a uniformly depolarized membrane. In our modeling we found no evidence of uncontrolled regenerative sodium current within the clefts between 10 and 300 ms that might masquerade as a slower inward current. This was illustrated both by the flatness of the recorded currents when the secondary inward current in the model of McAllister et al. was set to zero (Fig. 8, upper traces), and by the fact that, for the simulation, the voltage within the center of the fiber was within 5 mV of that on the surface during this time interval (unpublished). If the conductances of McAllister et al. are a valid representation of those in a Purkinje fiber, and if it is reasonable to approximate the geometry of the Purkinje fiber as we have done here, then it seems likely that radial nonuniformity would not represent a severe impediment toward recording the slow inward current in a 100-μm Purkinje fiber.

In these calculations we have not explored several additional consequences of the clefts. Because of the limited space, it is likely that accumulation and depletion of ions can occur, especially potassium (Baumgarten and Isenberg, 1977; Baumgarten et al., 1977). In addition to the effect this would have on the potassium driving force, it would also change the shape of the instantaneous rectifier curve for potassium. It is apparent, also, that increased fiber diameter will exaggerate the voltage nonuniformities and their consequences for current measurements in Purkinje fibers. This is because a larger fraction of the membrane is covert, and it is more difficult to control the cleft membrane near the center of the fiber. The results reported here should be considered appropriate only to fibers 100 μm or less in diameter.

The work was supported in part by U.S. Public Health Service grants HL 11665 and HL 20592.

Received for publication 3 May 1978 and in revised form 20 September 1978.

REFERENCES

ADRIAN, R. H., W. K. CHANDLER, and A. L. HODGKIN. 1969. The kinetics of mechanical activation in frog muscle. *J. Physiol. (Lond.).* **204**:207–230.

BAUMGARTEN, C. M., and G. ISENBERG. 1977. Depletion and accumulation of potassium in the extracellular clefts of cardiac Purkinje fibers during voltage clamp hyperpolarization and depolarization. *Pfluegers Arch. Eur. J. Physiol.* **368**:19–31.

BAUMGARTEN, C. M., G. ISENBERG, T. F. MCDONALD, and R. E. TENEICK. 1977. Depletion and accumulation of potassium in the extracellular clefts of cardiac Purkinje fibers during voltage clamp hyperpolarization and depolarization. Experiments in Na-free bathing media. *J. Gen. Physiol.* **70**:149–169.

DÉLÈZE, J. 1970. The recovery of resting potential and input resistance in sheep heart injured by knife or laser. *J. Physiol. (Lond.).* **208**:547–562.

DUDEL, J., and R. RÜDEL. 1970. Voltage and time dependence of excitatory sodium current in cooled sheep Purkinje fibres. *Pfluegers Arch. Eur. J. Physiol.* **315**:136–158.

EISENBERG, B., and L. D. PEACHEY. 1975. The network parameters of the t-system in frog muscle measured with the high voltage electron microscope. *In* 33rd Annual Proceedings of the Electron Microscopy Society of America. G. W. Bailey, editor. Claiter's Publishing Division, Baton Rouge, La.

FOZZARD, H. A. 1966. Membrane capacity of the cardiac Purkinje fibre. *J. Physiol. (Lond.).* **182**:255–267.

FOZZARD, H. A., and G. W. BEELER, JR. 1975. The voltage clamp and cardiac electrophysiology. *Circ. Res.* **37**:403–413.

GILAI, A. 1976. Electromechanical coupling in tubular muscle fibers. II. Resistance and capacitance of one transverse tubule. *J. Gen. Physiol.* **67**:343–367.

HELLAM, D. C., and J. W. STUDT. 1974*a*. A core-conduction model of the cardiac Purkinje fibre based on structural analysis. *J. Physiol. (Lond.).* **243**:637–660.

HELLAM, D. C., and J. W. STUDT. 1974*b*. Linear analysis of membrane conductance and capacitance in cardiac Purkinje fibres. *J. Physiol. (Lond.).* **243**:661–694.

LEDERER, W. J., and R. W. TSIEN. 1976. Transient inward current underlying arrhythmogenic effects of cardiotonic steroids in Purkinje fibres. *J. Physiol. (Lond.).* **263**:73–100.

MATHIAS, R. T., R. S. EISENBERG, and R. VALDIOSERA. 1977. Electrical properties of frog skeletal muscle fibers interpreted with a mesh model of the tubular system. *Biophys. J.* **17**:57–93.

MCALLISTER, R. E., and D. NOBLE. 1966. The time and voltage dependence of the slow outward current in cardiac Purkinje fibres. *J. Physiol.* **186**:632–662.

MCALLISTER, R. E., D. NOBLE, and R. W. TSIEN. 1975. Reconstruction of the electrical activity of cardiac Purkinje fibres. *J. Physiol.* **251**:1–59.

MOBLEY, B. A., and B. EISENBERG. 1975. Sizes of components in frog skeletal muscle measured by methods of stereology. *J. Gen. Physiol.* **66**:31–45.

MOBLEY, B. A., and E. PAGE. 1972. The surface area of sheep cardiac Purkinje fibres. *J. Physiol. (Lond.).* **220**:547–564.

NOBLE, D. 1962. A modification of the Hodgkin-Huxley equations applicable to Purkinje fibre action and pacemaker potentials. *J. Physiol. (Lond.).* **160**:317–352.

REUTER, H. 1967. The dependence of slow inward current in Purkinje fibres on the extracellular calcium concentration. *J. Physiol. (Lond.).* **192**:479–492.

REUTER, H., and H. SCHOLZ. 1977. A kinetic study of the ion selectivity and the kinetic properties of the calcium dependent slow inward current in mammalian cardiac muscle. *J. Physiol. (Lond.).* **264**:17–47.

SCHOENBERG, M., G. DOMINGUEZ, and H. A. FOZZARD. 1975. Effect of diameter on membrane capacity and conductance of sheep cardiac Purkinje fibres. *J. Gen. Physiol.* **65**:441–458.

SMITH, G. D. 1965. Numerical Solution of Partial Differential Equations. The Oxford University Press, London. 17–23.

SOMMER, J. R., and E. A. JOHNSON. 1968. Cardiac muscle: a comparative study of Purkinje fibers and ventricular fibers. *J. Cell Biol.* **36**:497–526.

TASAKI, I., and S. HAGIWARA. 1957. Capacity of muscle fiber membrane. *Am. J. Physiol.* **188**:423–429.

WEIDMANN, S. 1952. The electrical constants of Purkinje fibres. *J. Physiol. (Lond.).* **118**:348–360.